TERT promotor region rearrangements analyzed in high-risk neuroblastomas by FISH method and whole genome sequencing

Masumi Kawashima [a,b], Yuka Ueda [a,b], Sho Kurihara [a,b], Eiso Hiyama [a,b,c,□]

[a]Department of Pediatric Surgery, Hiroshima University Hospital, Hiroshima, Japan
[b]Graduate School of Biomedical & Health Science, Hiroshima University, Hiroshima, Japan
[c]Natural Science Center for Basic Research and Development (N-BARD), Hiroshima University, Hiroshima, Japan

*Corresponding author at: Natural Science Center for Basic Research, Hiroshima University,
1-2-3 Kasumi, Minami-ku, Hiroshima, 734-8551, Japan.
Tel.: +81 82 257 5951;
fax: +81 82 257 5416
E-mail address: eiso@hiroshima-u.ac.jp

Abstract

Background: Unfavorable neuroblastomas (NBLs) achieve telomere stabilization via telomerase activation through *MYCN* amplification, *TERT* promoter region (*TERT*-PR) rearrangements, or alternative telomere lengthening of telomeres. No well-established methods are available for investigating *TERT*-PR rearrangements. We examined the relationship between and prognosis by fluorescence *in situ* hybridization (FISH) upstream and downstream of *TERT* to establish a simple analysis method.

Procedure: *TERT*-PR rearrangements were analyzed in 3 M *MYCN* amplified cases, 2 M *MYCN* single cases, 1 MS case, 1 L2 case less than 18 months, and 1 L2 case over 18 months. Six patients with M and *MYCN* single were evaluated to determine if *MYCN* and *TERT*-PR rearrangement were independent prognostic factors. In total, 14 patients (11 males, 3 females; median age 36.4 months, range 1–122 months) with NBLs were evaluated at Hiroshima University. We identified *MYCN* amplification, *TERT* expression, and *TERT*-PR rearrangements. *TERT*-PR rearrangement was detected by FISH upstream and downstream of *TERT* on Chr5.p15.33. For *TERT*-PR rearranged cases, we characterized the fusion partners by whole genome sequencing.

Results: We detected *TERT*-PR rearrangements in two NBL samples. Both samples were high-risk NBLs and *MYCN* single NBLs, and their *TERT* expression levels were extremely higher than in the other samples. Genomic translocation occurred at chromosome 5p15.33 according to whole genome sequencing, agreeing with the FISH results. One case showed translocation of the chr5.p15.33 *SLCA6A19* gene to 22q12.3, and another case showed chr5p15.33 to chr5q33.3.

Conclusions: FISH is a useful diagnostic tool for evaluating high-risk NBLs in which *TERT*-PR rearrangements have occurred.

Keywords: *TERT*, Rearrangement, Neuroblastoma, Fluorescence *in situ* hybridization

1

1. Introduction

Neuroblastoma (NBL) is one of famous pediatric malignant tumor. Some NBL cases are in good prognosis as natural regression course, on the other hand, other NBL cases are poor course as life-threatening. It is known that the malignant grade of NBL mainly depending on the biological characteristics of the tumor cells.[1] *MYCN* amplification and chromosomal aberrations including 1p loss, 11q loss, and 17p gain have been reported as biological indicators as poor progressive factors.[2,3] In NBL, telomere shortening is correlated with NBL regression. Tumors with high telomerase activity are highly recurrent and associated with evaluating malignant grades.[4,5] Additionally, we previously reported that alternative lengthening of telomeres (*ALT*) is associated with unfavorable NBLs in older children without *MYCN* amplification.[4,6] Therefore, telomere stabilization by telomerase activation or *ALT* occurred in unfavorable tumors.[6,7] Studies of telomere biology have revealed several distinguishable NBL subtypes identified by telomere length and telomerase activation.[7-9] Recently, *TERT* promoter region (*TERT*-PR) rearrangements have been suggested as a distinguishable biological characteristic of NBLs,[10,11] and may be one of the major mechanisms of *TERT* activation in NBL.

Discriminating *TERT*-PR rearrangements by next generation sequencing and other similar methods is difficult and time-consuming.[12] Therefore, in this study, we developed a FISH-based method for detecting *TERT*-PR rearrangements.

2. Materials and Methods

2.1 Samples

NBL cases whose tumors were obtained before treatment at Hiroshima University Hospital or affiliated hospitals in Japan over the past two decades, the following 14 cases were selected as representatives in each risk group: 3 cases of International Neuroblastoma Risk Group Staging System (INRGSS) M *MYCN* amplified (NB294, 372, 322), 2 cases of INRGSS M *MYCN* non-amplified (NB384, 297), 1 case of INRGSS MS (NB454), 1 case of INRGSS L2 less than

18 months (NB351), and 1 case of INRGSS L2 over 18 months (NB275). Among these cases, *TERT*-PR rearrangement was observed in NB384, which was an INRGSSM and *MYCN* non-amplified case. Additional experiments were performed in six patients with INRGSS M and *MYCN* single to determine if *MYCN* and *TERT*-PR rearrangement are independent prognostic factors. These samples were obtained from patients who were followed up for longer than 2 years.

The mean age at initial diagnosis was 36.4 months (range, 1–122 months). Their clinical stages and histological findings were determined according to the INRGSS.[13] Written informed consent was obtained from all subjects or from their parents before surgery. This study was approved by the Institutional Review Board of Hiroshima University (I-RINRI-Hi-No.20).

NBL tumors were routinely examined for *MYCN* amplification by FISH or qualitative PCR analysis. Three cases were *MYCN*-amplified tumors.

Patients less than 12 months old with INRGSS L2 or MS disease were treated with either surgery or both surgery and chemotherapy. Patients 12 months or older with INRGSS L2 and M disease were typically treated according to the protocol described by the Japanese Children's Cancer Group.[14] Cases with INRGSS M tumor, except for some infants, were treated by myeloablative chemotherapy followed by bone marrow transplantation.

2.2 Primary culture of neuroblastoma cells

Fresh tumor tissue was disrupted into a single-cell suspension by manual homogenization using scissors, or simply scraping it on a plate surface. The suspended cells were cultured and then stored at -150℃ until use. The cells were thawed at room temperature and Puck's saline (0.4 g KCl, 0.35 g NaHCO$_3$, 8 g NaCl, 1 g D-glucose, 0.005 g phenol red, 2 mL 0.5 M EDTA) was added. After centrifugal separation at 1000 ×*g* for 5 min, the supernatant was discarded.

The cells were washed twice with phosphate-buffered saline and centrifuged at 1000 ×*g* for 5 min. Finally, the cells were

seeded into a flask containing RPMI medium (500 mL RPMI-1640 (Sigma-Aldrich, St. Louis, MO, USA) with 10% fetal bovine serum (FBS), 50 mL FBS, 5 mL antibiotic-antimycotic (100×) liquid)) or X-Medium (360 mL DMEM(Sigma-Aldrich) with 90 mL Medium199, 50 mL FBS, 5.06 mL antibiotic-antimycotic (100×)) and incubated at 37℃.

2.2 Analysis of TERT-PR rearrangements

2.2.1. FISH method

We custom-designed a SureFISH probe (Agilent Technologies, Santa Clara, CA, USA) approximately 400 kbp in length, which was labeled with Cy3 and Cy5 upstream and downstream of the *TERT* gene (Fig. 1).

We prepared primary cultured cells of the NBL samples, added colcemid (10 ng/mL), and placed the cells in an incubator at 37℃ for 90 min. The cells were collected and centrifuged at 4℃ 600 ×*g* for 5 min. After incubation, Carnoy solution (Wako, Osaka, Japan) (600 mL ethanol, 300 mL chloroform, 100 mL CH$_3$COOH) was added and the solution was centrifuged. The cells were placed on slides and stored at -80℃.

We performed FISH based on the Agilent FISH General Purpose Reagents protocol with overnight hybridization using non-formalin-fixed paraffin-embedded samples. The slides were placed sequentially in jars containing 70%, 85%, and 100% ethanol, with incubation for 1 min at room temperature in each jar. The probe and chromosomal DNA were denatured together at 78℃ for 5 min and hybridized overnight at 37 ℃ . Post-hybridization washing was performed using Agilent FISH Wash Buffer 1 (Agilent) for 2 min at 73℃ and with Agilent FISH Wash Buffer 2 for 1 min at room temperature. After washing in phosphate-buffered saline, Hoechst® 33342 (Thermo Fisher Scientific, Waltham, MA, USA) was added to the slide. Images were acquired using an Olympus Fluoview confocal microscope system (Tokyo, Japan).

2.2.2. Whole-genome sequencing

DNA was extracted from fresh-frozen tumor tissues with phenol/chloroform, precipitated with ethanol, resuspended in pH 8.0 TE buffer, and stored at 4°C.

Libraries were prepared using the TruSeq DNA PCR-free sample preparation kit (Illumina, San Diego, CA, USA) according to the manufacturers' instructions. The final libraries were sequenced on an Illumina HiSeq 2500 instrument, which produced paired-end 2 × 79 read lengths, with ≥640 M reads and ≥45 Gb data per sample.

2.2.3. Whole-genome sequencing date analysis

Raw sequencing reads were aligned to the human genome (NCBI build 37/hg19) and changes in rearrangement were analyzed by Strand NGS (Strand life Scientifics, Bangalore, India). Raw sequencing reads were aligned to the hg19 using BWA (version 0.7.15-r1140; https://github.com/lh3/bwa) followed by analysis of rearrangement changes using breakdancer-max[15] (version 1.4.5; https://github.com/genome/breakdancer) with default parameters. Rearrangements detected by both methods were manually filtered and validated by Sanger sequencing. PCR was performed on both the tumor tissue and patient's normal tissue, confirming that amplification was observed only in the tumor tissue.

A Circos plot representing the sequencing data was drawn by ClicO® (http://codoncloud.com:3000/). We deleted the line of the translocation date under 15 run-reads.

2.2.4. Quantification of *TERT* cDNA expression

Total RNA was extracted from fresh-frozen tumor tissues using an acid-guanidium phenol chloroform method as described previously. [11] Using a High-Capacity cDNA Archive kit (Applied Biosystems, Foster City, CA, USA), cDNA was extracted from these total RNA. *TERT* cDNA was quantitatively evaluated with master mix (Roche FastStart Universal Probe Master (ROX; Basel, Switzerland) using an ABI 7900HT FAST Real Time PCR system. For each sample, 2 μL cDNA (5 ng/μL), 0.4 μL SYG2076F primer, 0.4 μL SYG2097R primer, 0.35 μL ETL probe, and 2 μL *TERT* detection mix. RT–PCR for cDNA encoding the housekeeping gene GAPDH was processed in

a separate tube as a reference for relative quantification of *TERT* cDNA expression. A mixture without template was examined as the negative control. These mixtures were reverse-transcribed for 10 min at 95°C and the *TERT* cDNA sequence was amplified in 40 PCR cycles (15 s at 95°C and 60 s at 60°C) using specific primers in a one-step RT–PCR. To establish a standard curve, five standards with *in vitro*-transcribed *TERT* cDNA containing five different copy numbers were included in each experiment. The copy number of *TERT* cDNA in each sample was normalized based on the GAPDH cDNA content according to the formula: *TERT* cDNA expression level = *TERT* cDNA copies/GAPDH cDNA copies.

2.2.5. DNA sequencing of breakpoints

Rearrangements in the *TERT* locus were validated by Sanger sequencing. Sequencing was performed on both the tumor tissue and patient's normal tissue. PCR‐amplified products were then purified and subjected to direct sequencing using AmpliTaq Gold® (Thermo Fisher Scientific) with an automatic DNA sequencer (Applied Biosystems® ProFlex™ PCR System).

3. Results

3.1. Detection of *TERT*-PR rearrangements by FISH method

TERT-PR rearrangements were suspected in two NBL primary cultured cells by FISH. In the case of NB 384, in addition to the two points where green and red signals overlapped, a green point was detected separately (Fig. 2). In the case of NB 563, green and red signals overlapped at one point, whereas green and red were detected separately at another point, indicating a break point between the green and red probes (Fig. 2a). In other cases, only two points showed overlap of the green and red signals, suggesting that *TERT*-PR did not occur (Fig. 2b).

3.2. Analysis of *TERT*-PR rearrangement by whole genome sequencing

Genomic translocation was found at chromosome 5p15.33 in two NBL samples (NB384, NB563) by whole genome sequencing. In NB384, genomic translocation occurred on chromosome 5p15.33 in the *SLCA6A19* gene to 22q12.3. In NB563, genomic translocation occurred on chromosome 5p15.33 to 5q33.3 in the *BEF1* gene, 11 kb upstream from the *TERT* gene (Fig.3). We drew a Circos plot showing these genomic translocations (Fig. 4).

The fusion sequence in NB384 and NB563 was confirmed by PCR. Sequencing chromatograms of the Sanger sequence showed a break point (Fig. 5). These genomic translocation areas were amplified by PCR in the tumor samples but not amplified in normal tissues from the patient.

3.3. Clinical and biological features

We found *TERT*-PR rearrangements by FISH in two NBL samples (Fig. 2-a). TERT-PR rearrangements have been reported in approximately 25% of high-risk NBLs.[12] In our study, 10 patients diagnosed with INRGSS M, excluding NB 528 who was 7 months of age, were high-risk, and 2 of these patients had *TERT*-PR rearrangements. Therefore, *TERT*-PR rearrangements were detected in 2/10 cases (20%) of high-risk NBLs, which is lower than previously reported values.[10] In addition, *TERT*-PR rearrangements occurred only in *MYCN* non-amplified NBLs (2/11 cases, 18%).

TERT expression levels were 4513 and 5359 copies/GAPDH in cases positive for *TERT*-PR rearrangements, on the other hand from 0 to 139.5 (mean 53.6) in cases without *TERT*-PR. *TERT* expression tended to be higher in *TERT*-PR positive cases (Table 1, Fig. 6).

4. Discussion

Previous studies reported that *TERT*-PR rearrangements occurred in high-risk NBL.[11,12] However, there is no established method for investigating *TERT*-PR rearrangements of NBLs, various methods have been attempted, such as whole genome sequencing, single-nucleotide polymorphism detected, and PCR.[11,12,16]

Peifer et al. reported that break points were found in 5p15.33 by whole genome sequencing in high-risk NBL in

12/39 cases; 7 cases were translocated to chromosome 5 and 5 cases were translocated to other chromosomes.[12] As the position of translocation varies between cases, it is more difficult to detect TERT-PR rearrangements.

In the FISH method, the appearance of the fluorescence of probe differs depending on the translocation partners. The green and red probes were slightly separated in the translocation to chr5. In the case of translocation to another chromosome, the probe ahead of the break point appeared to be separated. If the break point was located in the green probe, green fluorescence appeared at one point apart; if the break point is in the red probe position, the red fluorescence appeared well separated. In our experiment, probes were designed to cover a wide area. FISH may be a useful method to detect these translocations in multiple area. If probe is designed to be short, the position of TERT-PR may be determined.

All cases where TERT-PR rearrangements were observed in our study were MYCN non-amplified tumors. TERT-PR rearrangements may be found in high-risk NBLs and more frequent in MYCN single cases than in amplified cases. In TERT-PR rearrangements cases, TERT expression was higher than in the other cases. MYCN is a known transcriptional activator of TERT.[17] TERT-PR rearrangements and MYCN amplification are independent TERT promotor activators, as TERT expression was increased despite MYCN single in cases of TERT-PR rearrangements. Therefore, TERT activation might be a driver for malignant transformation of NBLs and high expression of TERT is the most useful clinical indicator for unfavorable NBLs.

However, in our study, there was no obvious difference in prognosis between TERT-PR rearrangements cases and TERT-PR normal cases due to the low number of cases analyzed and insufficient follow-up period. At present, one of TERT-PR rearrangement cases died of disease and another is now alive with recurrent tumor, so that careful follow-up is required in this case. Future study is needed to analyze biological characteristics and outcomes of sufficient number cases with TERT-PR rearrangements

classified using this FISH method. In this study, we used primary culture cells derived from tumor tissues. To use this FISH method more applicable as clinical investigation, we have to examine this test in the stamp samples or FFPE (formalin-fixed and paraffin- embedded) samples of tumor tissues in the next step.

TERT-PR rearrangements have been studied in an abundance of tumor types.[18-23] TERT-PR mutation or TERT expression is involved in tumor incidence and progression. Examination of TERT-PR mutations and TERT expression is considered as useful for tumor diagnosis and determining a treatment plan. This may also be possible in childhood cancers such as neuroblastoma.

Recently, specific point mutations were described in the promoter region of the TERT gene in familial and sporadic melanoma and other cancers.[24] These point mutations lead to cytosine to thymine exchange at positions 228 or 250 upstream of the start codon of TERT and are named as C228T and C250T, respectively.[22-26] However, these mutations have not been reported in the primary tumor of NBL.[16] In our cases, the mutations were not recognized in NB384 and NB563 by whole genome sequencing. In NBLs, TERT is not activated by C228T and C250T. Therefore, easy and accurate evaluation of TERT-PR rearrangement is necessary.

FISH is a particularly useful diagnostic tool for high-risk NBL in which TERT-PR rearrangements are observed, whereas additional diagnostic assays may be necessary to identify compensatory mechanisms in TERT biology in NBL. Further studies are required to determine whether this method is useful for diagnosis in TERT-PR rearrangements. In our previous studies, high expression of telomerase activity has been shown to be correlated with advanced stages of disease and tumor biological features that predict a poor prognosis.[6,27,28] TERT expression levels are correlated with telomere activity levels.[6,25,26] TERT-PR rearrangement may be a major factor in upregulation of TERT expression levels.[29,30] MYCN amplification is an unfavorable factor,[2] and MYCN-amplified tumors typically exhibit high telomerase activity and high TERT

expression.[4,28] Telomerase activation often occurs by *TERT* activation through two pathways: *MYCN* amplification and rearrangement of the *TERT* promoter region. In addition, some NBLs had elongated telomeres, suggesting the existence of *ALT* by *ATRX/DAXX* mutations, which also led to a poor prognosis regardless of the telomerase activation status.[6,7] *ALT* mediates telomerase-independent telomere elongation.

NBLs are classified as favorable and unfavorable NBLs. In favorable NBLs, telomere length gradually shortens during cell division and then regresses or matures. In contrast, unfavorable NBLs acquire immortalization via telomere stabilization. Thus, telomere stabilization is key factor in NBL biology.

Studies of NBL biology are required to understand telomere biology, which may enable prognosis prediction and appropriate treatment based on the biological features of each tumor. *TERT*-PR rearrangement is one of the most important factors of NBL biology.

Disclosure statement

All authors have no conflict of interest.

References

[1] Gurney JG, Ross JA, Wall DA, et al. Infant cancer in the U.S.: histology-specific incidence and trends, 1973 to 1992. J Pediatr Hematol Oncol, 1997;19:428-432.

[2] Molenaar JJ, Koster J, Zwijnenburg DA, et al. Sequencing of neuroblastoma identifies chromothripsis and defects in neuritogenesis genes. Nature 2012;483(7391):589-593.

[3] Caron H, van Sluis P, de Kraker J, et al. Allelic loss of chromosome 1p as a predictor of unfavorable outcome in patients with neuroblastoma. N Engl J Med 1996;334(4):225-230.

[4] Hiyama E, Hiyama K, Yokoyama T, et al. Correlating telomerase activity levels with human neuroblastoma outcomes Nature Med 1995;1:249-255.

[5] Poremba C, Hero B, Heine B, et al. Telomerase is a strong indicator for assessing the proneness to progression in neuroblastomas. Med Pediatr Oncol 2000;35:651-655.

[6] Onitake Y, Hiyama E, Kamei N, et al. Telomere biology in neuroblastoma: telomere binding proteins and alternative strengthening of telomeres. J Pediatr Surg 2009;44:2258-2266.

[7] Kurihara S, Hiyama E, Onitake Y, et al. Clinical features of ATRX or DAXX mutated neuroblastoma. J Pediatr Surg 2014;49:1835-1838.

[8] Hiyama E, Hiyama K. Diagnostic and prognostic molecular markers in neuroblastoma. Kerala, Transworld research Network, 2009.

[9] Hiyama E, Iehara T, Sugimoto T, et al. Effectiveness of screening for neuroblastoma at 6 months of age: a retrospective population-based cohort study. Lancet 2008;371:1173-1180.

[10] Valentijn LJ, Koster J, Zwijnenburg DA, et al. TERT rearrangements are frequent in neuroblastoma and identify aggressive tumors. Nat Genet 2015;47:1411-1414.

[11] Kawashima M, Kojima M, Ueda Y, Kurihara S, Hiyama E. Telomere biology including TERT rearrangements in neuroblastoma: a useful indicator for surgical treatments. J Pediatr Surg 2016;51(12):2080-2085.

[12] Peifer M, Hertwig F, Roels F, et al. Telomerase activation by genomic rearrangements in high-risk neuroblastoma. Nature 2015;526(7575):700-704.

[13] Brisse HJ, McCarville MB, Granata C, et al. International Neuroblastoma Risk Group Project :Guideline for imaging and staging of neuroblastic tumors: consensus report from the International Neuroblastoma Risk Group Project. Radiology 2011;261:243-257.

[14] Sawaguchi S, Kaneko M, Uchino J, et al. Treatment of advanced neuroblastoma with emphasis on intensive induction chemotherapy: a report from the study Group of Japan. Cancer 1990;66:1879–1887.

[15] Fan et al. 2014 BreakDancer — identification of genomic structural variation from paired-end read mapping. Curr Protocol Bioinformatics 2014;45:15.6.1-15.6.11.

[16] Lindner S, Bachmann HS, Odersky A, et al. Absence of telomerase reverse transcriptase promoter mutations in neuroblastoma. Biomed Rep 2015;3(4):443-446.

[17] Mac SM, D'Cunha CA, Farnham PJ. Direct recruitment of N-myc to target gene promoters. Mol Carcinog 2000;29(2):76-86.

[18] Huang M, Yan C, Xiao J, et al. Relevance and clinicopathologic relationship of BRAF V600E, TERT and NRAS mutations for papillary thyroid carcinoma patients in Northwest China. Diagn Pathol 2019;14(1):74.

[19] Stenman A, Hysek M, Jatta K, et al. TERT promoter mutation spatial heterogeneity in a metastatic follicular thyroid carcinoma: implications for clinical work-up. Endocr Pathol 2019;30(3):246-248.

[20] Giorgenon TMV, Carrijo FT, Arruda MA, et al. Preoperative detection of TERT promoter and BRAFV600E mutations in papillary thyroid carcinoma in high-risk thyroid nodules. Arch Endocrinol Metab 2019;63(2):107-112.

[21] Lu VM, Goyal A, Lee A, et al. The prognostic significance of TERT promoter mutations in meningioma: a systematic review and meta-analysis. J Neurooncol 2019;142(1):1-10.

[22] Amisaki M, Tsuchiya H, Sakabe T, et al. Identification of genes involved in the regulation of TERT in hepatocellular carcinoma. Cancer Sci 2019;110(2):550-560.

[23] Gay-Bellile M, Véronèse L, Combes P, et al. TERT promoter status and gene copy number gains: effect on TERT expression and association with prognosis in breast cancer. Oncotarget 2017;8(44):77540-77551.

[24] Horn S, Figl A, Rachakonda PS, et al. TERT promoter mutations in familial and sporadic melanoma. Science 2013;339:959‑961.

[25] Griewank KG, Murali R, Schilling B, et al. TERT promoter mutations in ocular melanoma distinguish between conjunctival and uveal tumours. Br J Cancer 2013;109:497‑501.

[26] Huang FW, Hodis E, Xu MJ, et al. Highly recurrent TERT promoter mutations in human melanoma. Science 2013;339:957‑959.

[27] Reynolds CP, Zuo JJ, Hong CM, et al. Telomerase RNA expression in neuroblastoma correlates with high stage and clinical outcome. Proc Amer Assoc Cancer Res 1996;37:199.

[28] Hiyama E, Hiyama K, Ohtsu K, et al. Telomerase activity in neuroblastoma: is it prognostic indicator of clinical behavior? Eur J Cancer 1997;33:1932–1936.

[29] Greenberg RA, O'Hagan RC, Deng H, et al. Telomerase reverse transcriptase gene is a direct target of c-myc but is not functionally equivalent in cellular transformation. Oncogene 1999;18:1219–1226.

[30] Kyo S, Takakura M, Taira T, et al. Sp1 cooperates with c-myc to activate transcription of the human telomerase reverse transcriptase gene (hTERT). Nucleic Acids Res 2000;28:669–677.

Table1. Neuroblastoma cases

Case	Age at Dx(mo.)/gender	Origin	INRGSS	Outcome	MYCN	TERT(/GAPDH)	TERT-PR rearrangement
NB384	36/F	mediastinal	M	DOD(25mo.)	S	5359	+
NB294	38/M	adrenal	M	NED	A	71.1	
NB297	41/M	adrenal	M	NED	S	106.3	
NB372	29/M	adrenal	M	DOD(22mo.)	A	8.1	
NB351	1/M	adrenal	L2	NED	S	13.1	
NB454	3/M	adrenal	MS	NED	S	37.6	
NB275	20/F	adrenal	L2	NED	S	100.8	
NB322	14/M	retroperitoneal	M	DOD(0mo.)	A	139.5	
NB480	62/F	retroperitoneal	M	DOD(79mo.)	S	28.7	
NB526	38/M	adrenal	M	DOD(20mo.)	S	77.2	
NB528	7/M	retroperitoneal	M	DOD(5mo.)	S	0	
NB544	30/M	mediastinal	M	NED	S	50.8	
NB552	122/M	retroperitoneal	M	DOD(17mo.)	S	10.1	
NB563	66/M	retroperitoneal	M	NED	S	4513	+

DX: diagnosis, M:male, F: female, mo. Months of age, INSS: International Neuroblastoma Staging System, TERT: telomerase reverse transcriptase, PR: promotor,

DOD: dead of disease, NED: no evidence of disease.
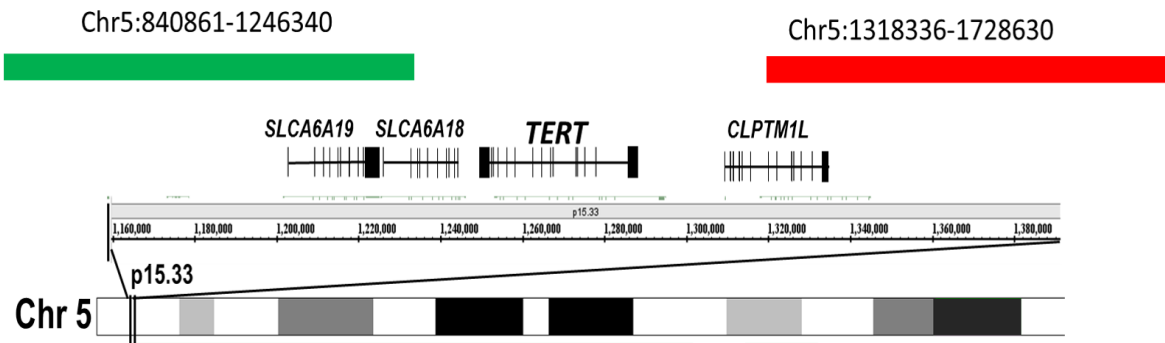
S: single, A: amplified.

Figure

Fig.1. Probe design in FISH protocol

Probes with Cy3 (green line) and Cy5 (red line) were designed upstream and downstream of the *TERT* gene.
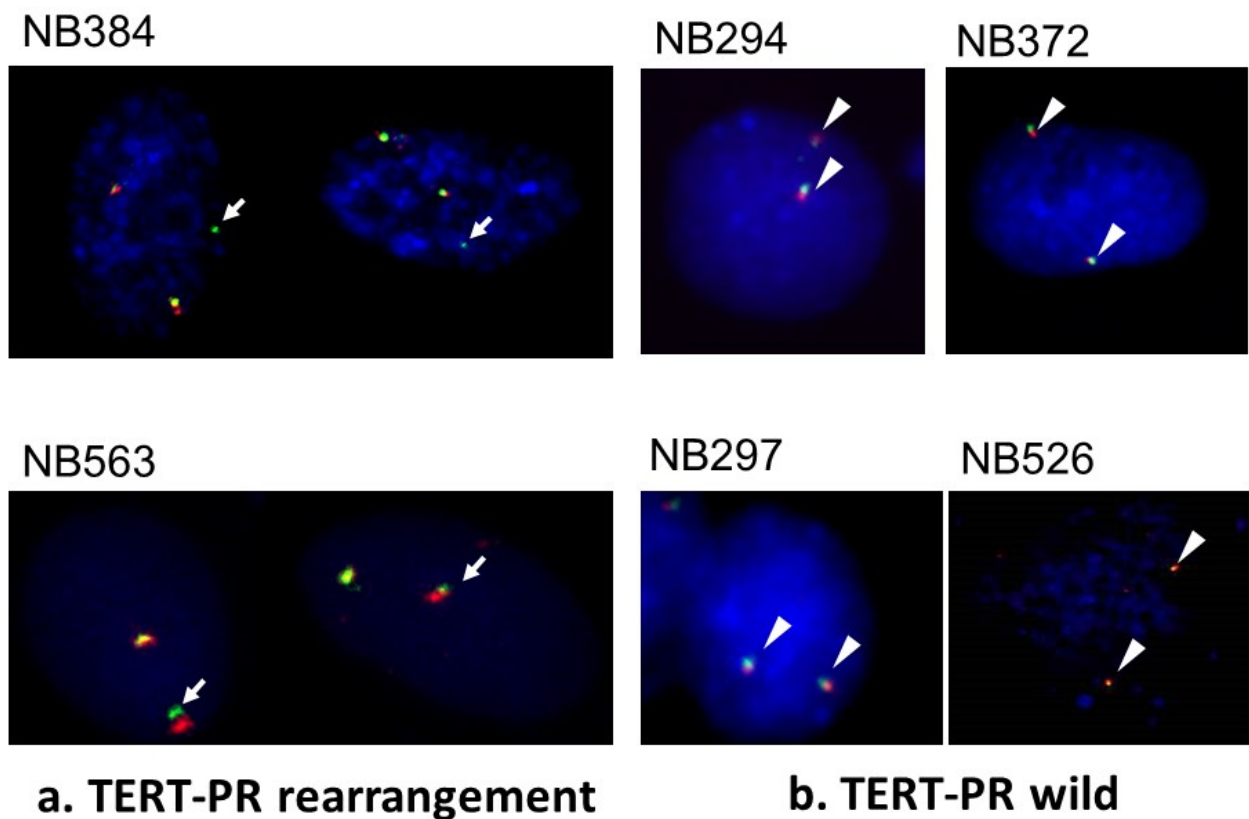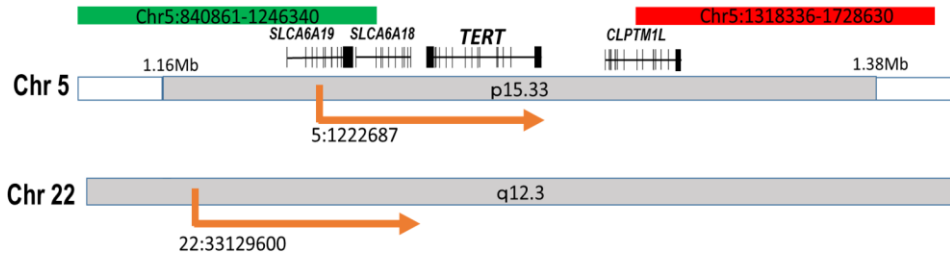

a. TERT-PR rearrangement b. TERT-PR wild

Fig2. Detection of *TERT*-PR rearrangements by the Break Apart FISH method

Arrows indicate *TERT*-PR rearrangements (green signals without adjacent red signals) in Fig2-a (NBs 384 and 563)-2.

Arrowheads indicate *TERT*-PR normal (green signals in close proximity to red signals)in Fig. 2-b (NBs 294, 297, 372, and .526)
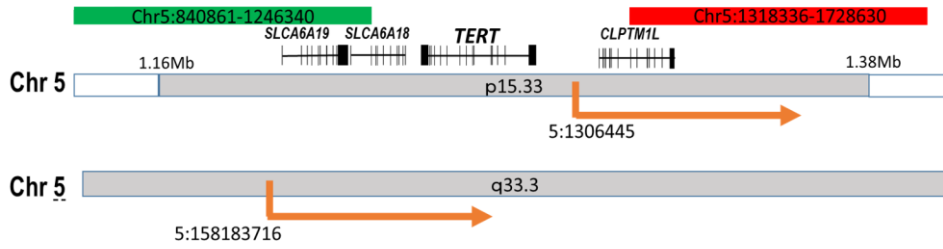
Fig3. Image of genomic translocation

a. Genomic translocation was detected in NB384. The break point were located at chromosome 5p15.33 and in green probe range.

b. Genomic translocation was detected in NB563. The break point were located at chromosome 5p15.33 and between green and red probe.
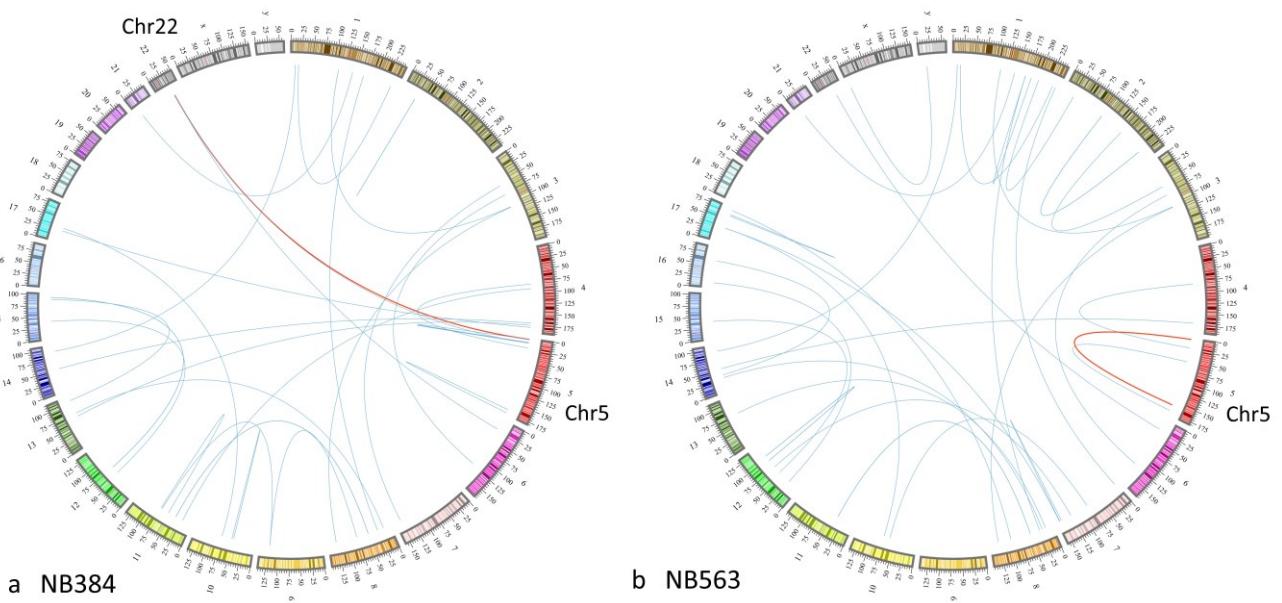

Fig4. Schematic representation of the genomic translocations in NB384 and NB563

a, Circos plots showing genomic translocation occurred in NB384 tumors detected by BreakDancer. Red plot line shows rearrangement on chromosome 5p15.33 *SLCA6A19* gene to 22q12.3 at FISH region.

b, Circos plots showing genomic translocation occurred on chromosome 5p15.33 to 5q33.3 *BEF1* gene in NB563 tumors.
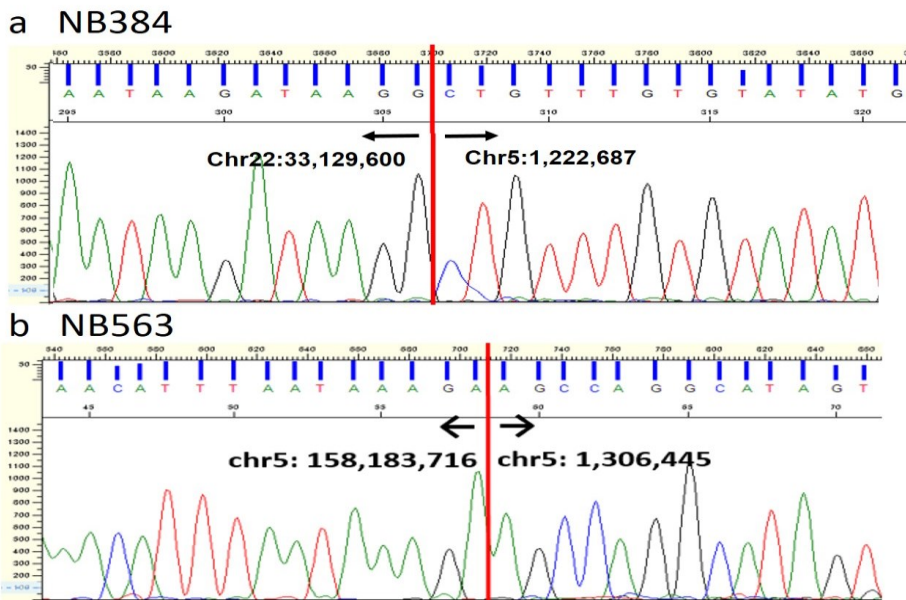
Fig5. Validation of rearrangements of the *TERT*-PR lesion by sanger sequencing.

a, Sequencing chromatogram of sanger sequence shows the breakpoint between chromosome 5p15.33 *SLCA6A19* gene to 22q12.3. in NB384 tumor.

b, Sequencing chromatogram of sanger sequence shows the break point is between Exon10 to 11 of *EBF1* gene inNB563 tumor.
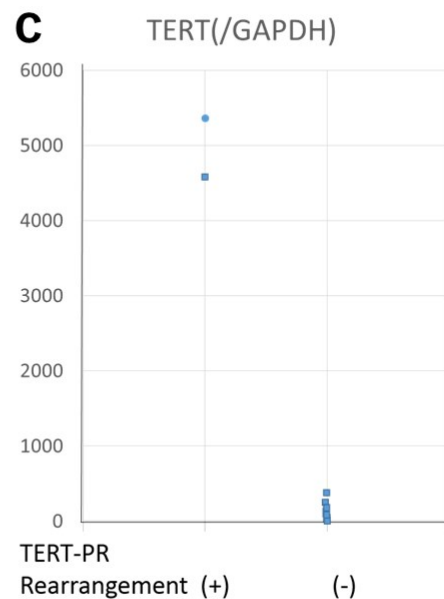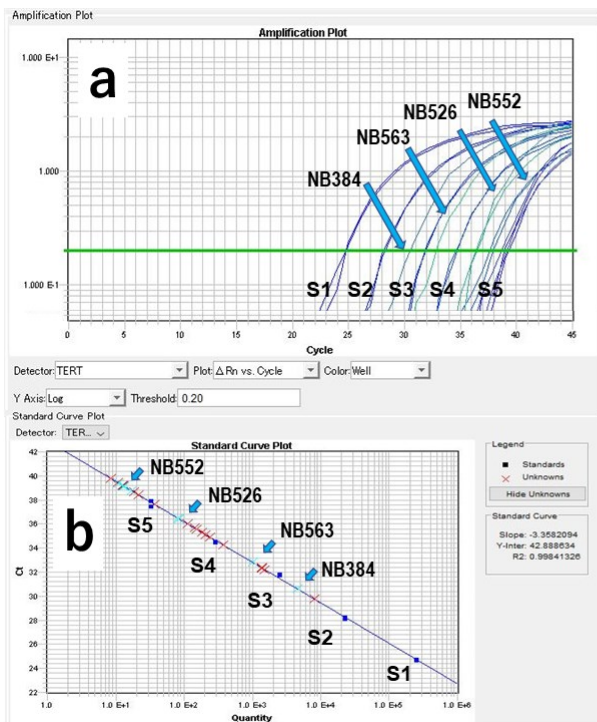

Fig6. Detection of TERT mRNA expression analysis using real time RT-PCR

a. Amplification plots of TERT in the standard and NBL samples. The products of NB 384 and NB 563 samples shows the low Ct values and others shows the high Ct values. (Thresfold: 0,20) .

b. Standard curve plot of this RT-PCR. The amounts of TERT mRNA were estimated using this plot.

c. Comparison of TERT mRNA expression levels of NBL samples with or with out TERT-PR rearrangements. The TERT mRNA expression levels were corrected by those of internal standard (GAPDH). The TERT expression were obviously up-regulated in the TERT-PR rearranged NBL samples.

11